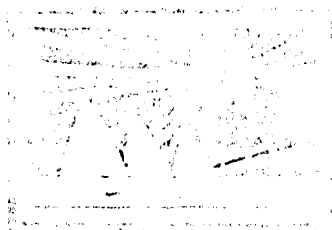


EG 9401247

A.R.E.A.E.E./Rep. — 282



ARAB REPUBLIC OF EGYPT
ATOMIC ENERGY ESTABLISHMENT
DEPARTMENT OF METALLURGY

HIGH TEMPERATURE HIGH VACUUM CREEP
TESTING FACILITIES

By

M.K. MATTA

1985

NUCLEAR INFORMATION CENTER
ATOMIC ENERGY POST OFFICE
CAIRO, A.R.E.

We regret that some of the pages in the microfiche copy of this report may not be up to the proper legibility standards, even though the best possible copy was used for preparing the master fiche.

Page 18 missing!

ARAB REPUBLIC OF EGYPT
ATOMIC ENERGY ESTABLISHMENT
NUCLEAR METALLURGY DEPARTMENT

HIGH TEMPERATURE HIGH VACUUM CREEP
TESTING FACILITIES

BY
M.K. MATTA

1985
NUCLEAR INFORMATION DEPARTMENT
ATOMIC ENERGY POST OFFICE
CAIRO, A.R.E

ACKNOWLEDGMENTS

I would like to acknowledge my debt and gratitude to Prof. Hans Ullmaier, Head of the Mechanical Testing and Radiation Damage group in IFF-Jülich for his support to manufacture these machines in IFF Workshop and for his encouragement and learned advice during the manufacture process. My heart felt thanks to Dr. Herbert Schroeder and Mr. Joseph Deutz of IFF-KFA Jülich for their helpful discussions, technical help and constant advice.

The machines were constructed in the frame work of bilateral agreement between the Institut Für Festkörperforschung "IFF- of the Kernforschungsanlage "KFA" Jülich West Germany and the Nuclear Metallurgy Department of the Egyptian Atomic Energy Authority. The agreement was signed in July, 1981 between Prof. Hans Ullmaier and Dr. Ahmed A. Abou Zahra. The assistance of the KFA International Bureau in this regard is highly acknowledged.

I wish to record my sincere thanks and gratitude to Prof. F.H. Hammad, Head of the Metallurgy Department, Nuclear Research Centre, Atomic Energy Authority for his advice, helpful discussions, keen interest during writing this report and for a critical reading of the manuscript.

CONTENTS

	Page
ACKNOWLEDGMENTS	Page
ABSTRACT.....	ii
I. INTRODUCTION.....	1
1.1. General Introduction.....	1
1.2. Creep and its Importance in Nuclear Technology.....	2
1.2.1. Stages of creep.....	2
1.2.2. The effect of temperature.....	5
1.2.3. The effect of stress.....	7
1.2.4. Creep rupture.....	8
II. TECHNICAL DESCRIPTION OF THE CREEP MACHINE.....	9
II.1. Introduction.....	9
II.2. Detailed Description of the Machine.....	9
II.2.1. Vacuum system.....	9
II.2.2. Creep column.....	12
II.2.3. Specimen holder and temperature measurements.....	14
II.2.4. The load system.....	18
II.2.5. Elongation measurements and recording	18
III. CREEP BEHAVIOUR OF HELIUM IMPLANTED STAINLESS STEEL.....	23
III.1. Experimental procedure.....	23
III.1.1. Sample preparation.....	23
III.1.2. Helium implantation.....	24
III.1.3. Creep tests.....	24
III.2. Results and Discussion of Creep Data.....	24
REFERENCES.....	32

ABSTRACT

Creep is the term used to describe time-dependent plastic flow of metals under conditions of constant load or stress at constant high temperature. Creep has an important considerations for materials operating under stresses at high temperatures for long time such as cladding materials, pressure vessels, steam turbines, boilers....etc.

These two creep machines measures the creep of metals and alloys at high temperature under high vacuum at constant stress. By the two chart recorders attached to the system one could register time and temperature versus strain during the test.

This report consists of three chapters. Chapter I is the introduction, chapter II is the technical description of the creep machines while chapter III discuss some experimental data on the creep behaviour, of Helium Implanted Stainless Steel.

INTRODUCTION

1.1. General Introduction:

During my stay from February, 1981 to July, 1982 as a guest scientist in the Institut Für Festkörperforschung "IFF" of the Kernforschungsanlage "KFA" Jülich, West Germany and beside my scientific research programme I constructed two high vacuum high temperature creep machines. The IFF has donated them to the Metallurgy Division of the Egyptian Atomic Energy Establishment in the frame work of bilateral collaboration. During my stay I have supervised the manufacture of the two creep machines in the IFF workshops, the installation process, calibration testing then dismantling for shipping to Egypt. I also supervised receiving them in Egypt and I took the responsibility of installing and putting them in working conditions again in the Laboratories of Metallurgy Department at Nuclear Research Centre at Inchass.

This machine is highly advanced and utilizes an accurate technique to measure and record the creep of metals at constant stress under high vacuum and at high temperatures.

Introducing such machines in the Metallurgy Department will intensify the continuation of the collaboration between both Laboratories through the exchange of data obtained and scientific visits between the scientists of both countries. By introducing such a highly advanced creep machines will enables us to use a new technology of studying the creep behaviour of metals and alloys of nuclear applications e.g. stainless steels, zirconium, and zirconium alloys. As a matter of fact this equipment is considered to be the first machine of its type introduced in the Atomic Energy Authority.

1.2 Creep and Its Importance in Nuclear Technology:

Creep is the term used to describe the time dependent plastic flow of metals under conditions of constant load or stress. Whilst creep can occur over the whole temperature range and has been observed down to liquid helium temperatures, with engineering metals and alloys creep is of practical importance only at high temperatures. During the last quarter of a century, there has been a marked expansion in the requirements for materials operating at high temperatures where creep is an important consideration. This expansion arises from the growth of various specialised engineering activities, such as the development of high temperature gas-cooled reactors and gas turbines, plus the increasing demands placed on more conventional components such as boilers, steam turbines, and pressure vessels. The increasing importance of high-temperature metallurgy has led to considerable development of improved materials, largely by optimisation of existing alloy types. Increasing technological requirements have also led to much closer examinations into the long term properties e.g. creep of alloys. This promotes proper optimisation of design and fuller utilisation of available metals and alloys.

1.2.1. Stages of Creep:

Whilst the mechanical behaviour of metals is usually described adequately for engineering purposes by the stress-strain diagram, creep is more conveniently shown by strain-time curves at constant temperature and stress. Typical creep curves are shown schematically in Figure 1. In the general case there are three stages in a creep curve, in addition to a preliminary stage which consists of

the almost instantaneous deformation occurring during the application of the load. In stage I the creep rate decreases continually with time, representing a period of work hardening, or increasing resistance to creep. This stage is usually termed primary or transient creep. The next stage, known as secondary or steady-state creep, is most important stage of creep for many industrial applications; it represents a period where the material creeps at constant rate. This stage, shown as II in Figure 1 may last for many years and is thought to represent a period of balance between work hardening and recovery processes. It leads eventually to stage III, or tertiary creep, which is a period of increasing creep rate terminated by rupture. This final period is often associated with growth of microcracks in the material.

Whilst the three-stage creep curve described is the one most commonly observed, other forms of strain-time plots are seen occasionally. Sometimes, the creep rate increases progressively almost from the onset of testing, particularly when high stresses are used. In other cases, creep rates appear to continually decrease, ultimately terminating in tertiary creep and failure; i.e. no true secondary creep is observed. Such instances are often associated with structural instabilities in materials which are either softening or hardening during the course of testing, thus eliminating the steady-state condition of creep. In most engineering applications where creep is of importance, components are required to last for many years without failure, Such components include rotors, chests, casings and blades in turbines, steam pipes in boilers, fuel element supports in nuclear

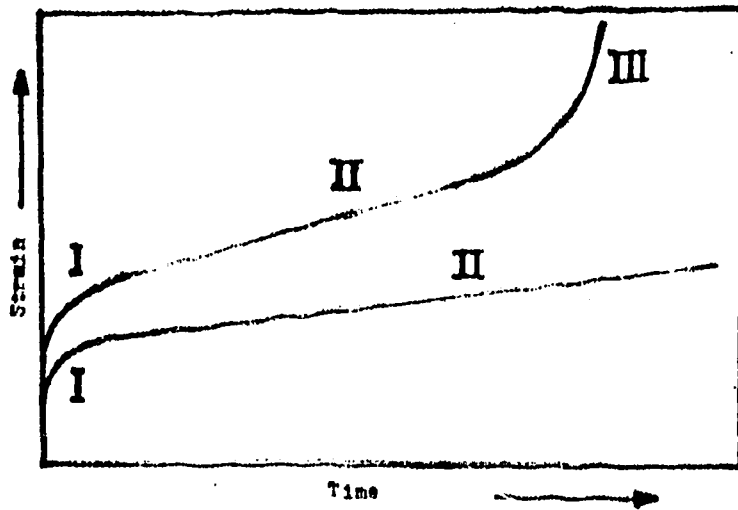


Figure I Typical creep curves.

reactors, high-temperature pressure vessels and many other components which are required to operate for long periods at elevated temperatures. For such applications, the behaviour of materials during primary creep is of only marginal importance. Primary creep is usually complete after at most, a few hundred hours. Provided the strain occurring during this primary stage is not excessive, it is the secondary creep behaviour, coupled with the rupture strain, that largely dictates the working stress and temperatures of various materials.

1.2.2. The Effect of Temperature:

Creep is principally a high-temperature phenomenon in most engineering materials. The temperature at which creep becomes important is, in fact, related to the melting point of the alloy concerned. Creep deformation does occur at low temperatures, but for all practical purposes is of little importance between the absolute zero in temperature and $0.3 T_m$, where T_m is the melting point in degrees absolute. As the temperature is raised above $0.3 T_m$, creep must be increasingly reckoned.

Steel has a melting point of around 1500°C (1773°A) and creep is unlikely to become a problem until temperatures in excess of around 300°C are reached. While melting point has a large influence on creep characteristics, it is only one of many important factors to be considered. Crystallographic and metallurgical structure can also play a large part in the temperature at which creep becomes important. For instance, while creep becomes important in body - centered cubic ferritic steels above 300°C , in face - centred cubic

austenitic stainless steel, creep is of little importance until 500°C has been exceeded, despite the similarity in melting point, of the ferritic and austenitic steels. The relationship between melting point and creep resistance is only a rough guide which can be influenced markedly by other factors. Creep deformation is a thermally activated process which is controlled by the well known Arrhenius equation:-

$$\dot{\epsilon} = A \exp (- Q/RT)$$

where $\dot{\epsilon}$ is the creep rate, Q is the activation energy for creep, T is the absolute temperature and R is the gas constant. Increasing a small temperature, therefore, produces an exponential increase in creep rate. Thus, in iron, for instance, with an activation energy of 70,000 cal/mol, an increase in temperature from 350°C will produce a 65-times increase in creep rate at constant stress. Activation energies, Q, have been measured for many systems. The measurement which is relatively simple, can be made typically by abruptly changing the test conditions of a creep test from stress 1, temperature T₁, to stress 2, temperature T₂. Allowing for various assumptions, the activation energy can then be computed from the change in creep rate by the expression:

$$Q = \frac{R \ln \dot{\epsilon}_1 / \dot{\epsilon}_2}{\frac{1}{T_2} - \frac{1}{T_1}}$$

Examination of measured activation energies for creep has shown that at temperatures above 0.5 T_m they bear a remarkable similarity to the activation energies for atomic self-diffusion in pure metals. In the case of alloys, creep

activation energies usually equal the activation energy for diffusion of one of the elements. Therefore at high temperature creep is governed by mechanisms controlled by atomic self-diffusion.

1.2.3. The Effect of Stress:

It is well established that creep rates are very dependent on the stress, and there is considerable evidence to show that under most circumstances the secondary creep rate of metals is affected by a power function of the stress. This can be represented by the equation:

$$\dot{\epsilon} = K \sigma^n$$

where $\dot{\epsilon}$ is the strain rate, σ is the stress and K and n are constants. It has been found that for pure metals and many alloys, n equals 3-5, and creep behaviour in the large majority of cases can be classified as having stress indices within this range. This means that if the creep stress is doubled, creep rates will usually increase somewhere between 8 and 32 times.

As stresses are increased the relationship $\dot{\epsilon} = K \sigma^n$ breaks down and the stress dependence of creep becomes $\dot{\epsilon} = A \exp(B\sigma)$ where A is a constant and B constant of about 10 for equiaxial polycrystals whilst this is often quoted as a secondary creep relationship at high stresses, it seems quite possible that at the strain rates and stresses where this relationship is said to apply, true secondary rates are never observed, and tertiary creep is operating.

1.2.4. Creep Rupture:

As described earlier, in the last stages of creep the strain rate accelerates rapidly to failure, and this has been ascribed in macroscopic terms to the increasing stress arising during local reductions in the cross-sectional area of the specimen. Such an explanation, however, is something of a gross over-simplification; tertiary creep has often been observed prior to the formation of a visible neck in the material. Tertiary creep and failure can, in fact, be associated with the growth of micro-cracks or voids in the material which can be developed long before local reductions in cross-section occur.

Under slow strain rate, high temperature conditions, fracture is usually intergranular with a corresponding loss in ductility. It is known that significant amounts of grain boundary sliding occur during creep, the ratio of grain boundary slide to total strain increasing as the strain rate is lowered and the temperature is raised. Very often, therefore, as the time to failure increases, so the rupture mode becomes intergranular and the rupture strain falls. In addition, as strain is concentrated in grain boundary regions, a coarse grain size leads to lower rupture strains than does a fine grain size.

Metallographic studies of initiation and propagation of intergranular creep cracks have established that during creep, cavities develop along grain boundaries and wedgeshaped cracks form at grain boundary triple points. Growth and linking of such cavities and cracks eventually lead to failure.

II- TECHNICAL DESCRIPTION OF THE CREEP MACHINE

II.1. Introduction:

The machine is composed of two units and Fig.2 shows a photograph for them. Unit I includes the vacuum pumps, the two creep columns with their furnaces all are installed in an iron frame of folding type to facilitate the transportation problem. This iron frame is of dimensions 170x100x75cms. While unit II, includes the control panel which is fixed on an iron frame of dimensions 170 x 55 x 70 cms. The base of that frame is movable by four wheels each of diameter 8 cm. The control panel consists of the vacuum meters for measuring mechanical and high vacuum, the four channel carrier frequency measuring amplifier, the two temperature controllers & a ventilator with two small horizontal fans ^{to} cool down the above mentioned equipment during the long term tests. The two chart recorders to record the elongation and temperature versus time for each column.

II.2. Detailed Description of the Machine

II.2.1. Vacuum system:

Figure 3 shows a Leybold Heraeus mechanical pump 220 V, 50 Hz, 250 W and 1400 turn/min. By the mechanical pump we could reach to 10^{-3} Torr. For high vacuum till 10^{-6} Torr a 180 model Leybold Heraeus diffusion pump is connected to the mechanical pump. The mechanical vacuum can be measured by Alcatel ATH21 and the high vacuum by Alcatel ACF10 vacuum meter. All components of this apparatus are made of leak proof stainless steel joints. The junctions are connected with copper gaskets.

To avoid overheating of silicon oil of the diffusion pump a safety valve is connected to it so that in case if the flow of water is reduced than the permissible rate-

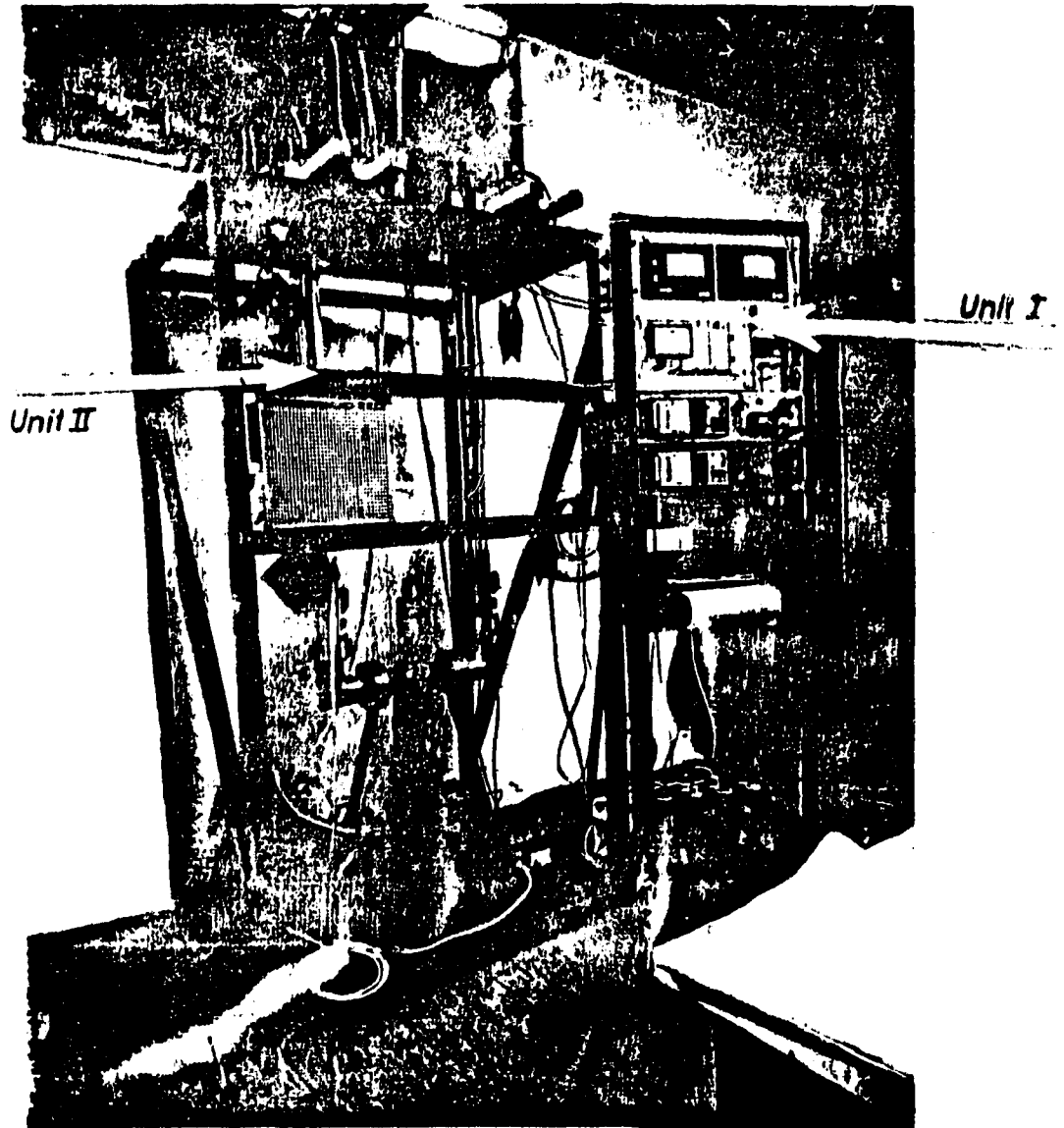


Fig. 2 Shows the two units of the creep machine

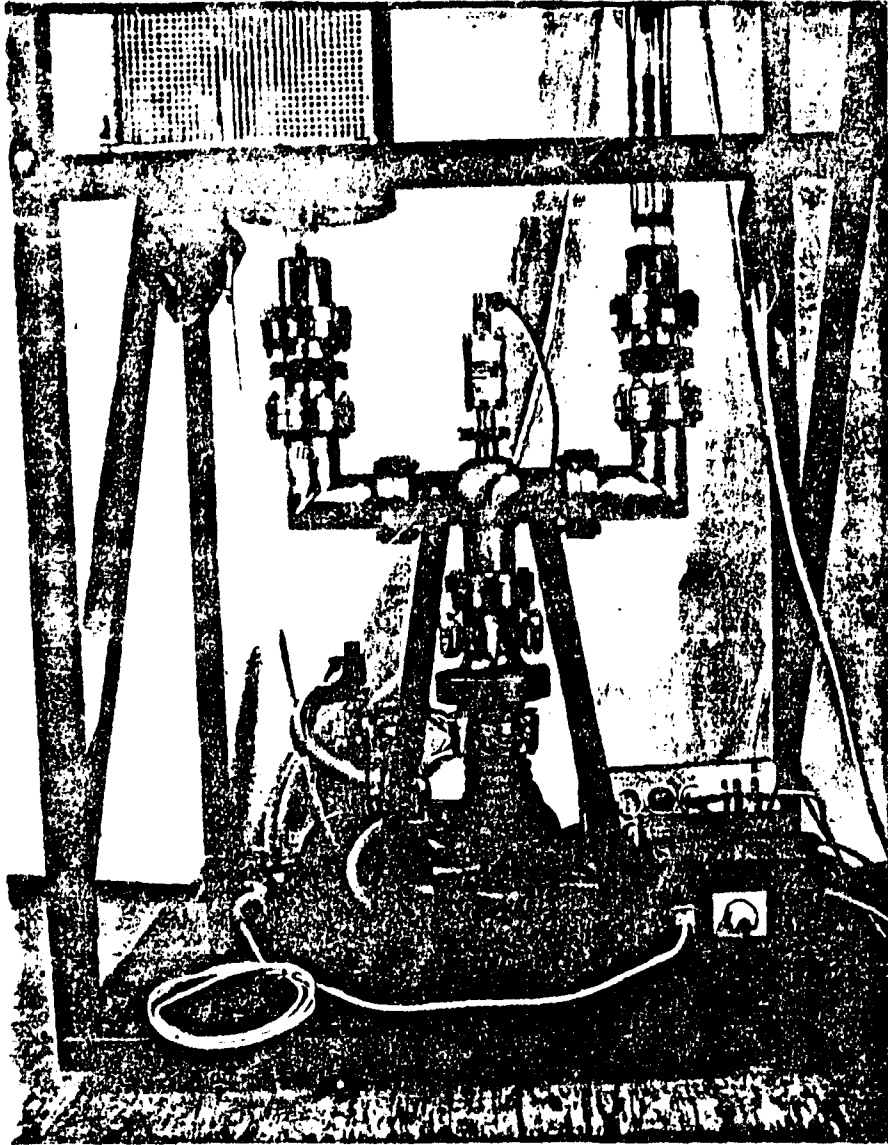


Fig. 3 Illustrating the vacuum system

15 litre/ hour-the valve switches off the power automatically from the diffusion pump heater.

For metals which have high oxygen affinity at high temperatures these two creep machines can be used under vacuum otherwise for less oxygen affinity metals they can be tested in open air.

II.2.2. Creep column:

Figure 4 shows the creep column which is mounted on a Leybold Heraeus CF63 UHV flange of diameter 11.2 cm. It is thus be able to be placed vertically inside a transparent quartz tube of 70 cm length, and interior diameter is 58 mm with wall thickness of 3 mm. The upper and lower ends of the quartz tube are connected to stainless steel tubes of 6 cm long each. They are sealed to the quartz tube by using UHU Plus Endfest 300. For each quartz tube the upper and lower stainless steel end is connected to Leybold Heraeus ultra high vacuum flange. Since there are always residual stresses at the junctions therefore these are mechanically unstable, for this reason the quartz tubes are connected to the apparatus by metallic spring bellows at the top and a metallic membrane bellows at the bottom, both the spring and the membrane are leak proof.

Figure 4 shows the creep column assembly which is made of stainless steel and can be briefly described as follows: Two stay bars of about 80 cm length and 8 mm diameter are welded on to a CF63 UHV flange. A bottom plate 10 mm thick is attached to the end of the stay bars and supports the lower part of the specimen holder via a threaded rod 2 mm thick. The upper portion of the specimen holder hangs from a tension spring via a tension rod 2 mm thick in diameter is made from molybdenum which has a high

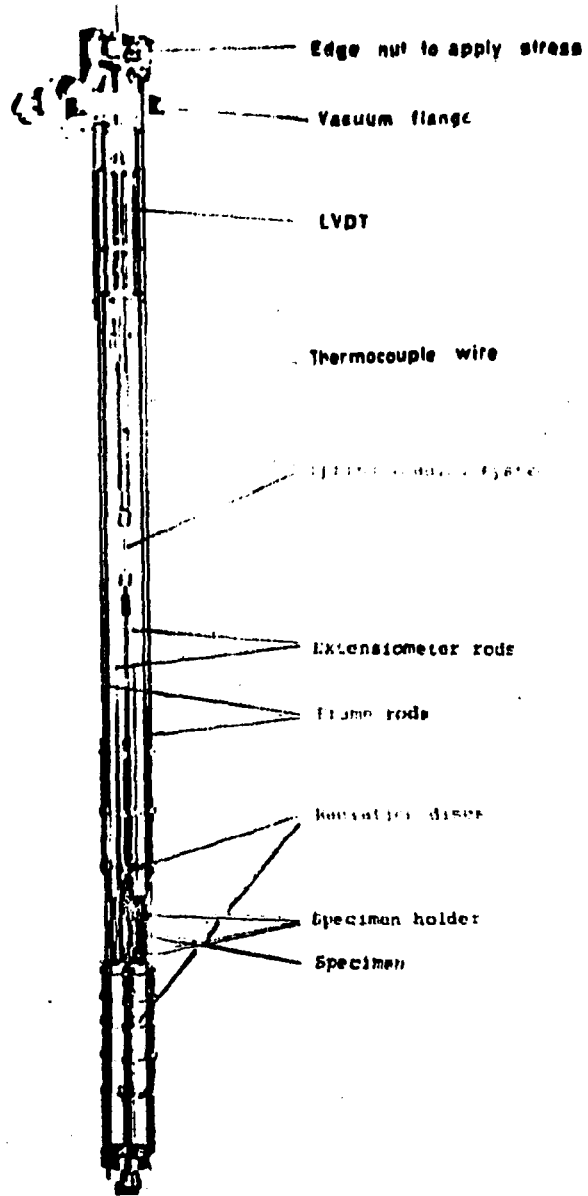


Fig.4 The creep column assembly.

creep resistance at the test temperature range from 600-900°C. This spring can be stretched by turning the upper knurled nut and load thus applied to the specimen. In order to reduce the temperature gradient inside the quartz tube, stainless steel radiation discs were mounted in the upper and lower regions of the specimen. For further reduction of the temperature gradient directly at the specimen a stainless steel cylinder (inner diameter 30 mm, 1 mm thick and 50 mm length) surrounding the specimen. Thus a temperature gradient of less than 3°C resulted inside this cylinder.

II.2.3. Specimen holder and temperature measurements:

Figure 5 shows the schematic representation of a creep specimen which is in a sheet form of 0.1 - 0.15 mm thick. The most convenient stainless steel specimen holder was constructed for reasons of limited space and the load measurement should not be distorted. It was rather difficult to clamp the thin specimens of 100 - 150 μ m thick. Only a very carefully constructed clamping jaws could stop the specimens from slipping from the holder. Fig.6a shows a creep sample mounted in the specimen holder outside the creep machine while Fig. 6b shows the same sample mounted in the specimen holder and fixed on the creep machine.

Regarding heating system, for each creep column a Heraeus tubular furnace opened from both ends of the type ROK/A-6/30 with maximum temperature 1100°C, inner diameter 60 mm, 300 mm long, 220 V, 2.5 KW and 50 Hz is used. The furnaces are vertically fixed in such a way that they are surrounding the quartz tubes from outside and the creep samples are adjusted so that it should lie at the centre of the hot zone of each furnace. A Ni Cr-Ni thermocouple is used to measure the temperature at the centre of the gauge

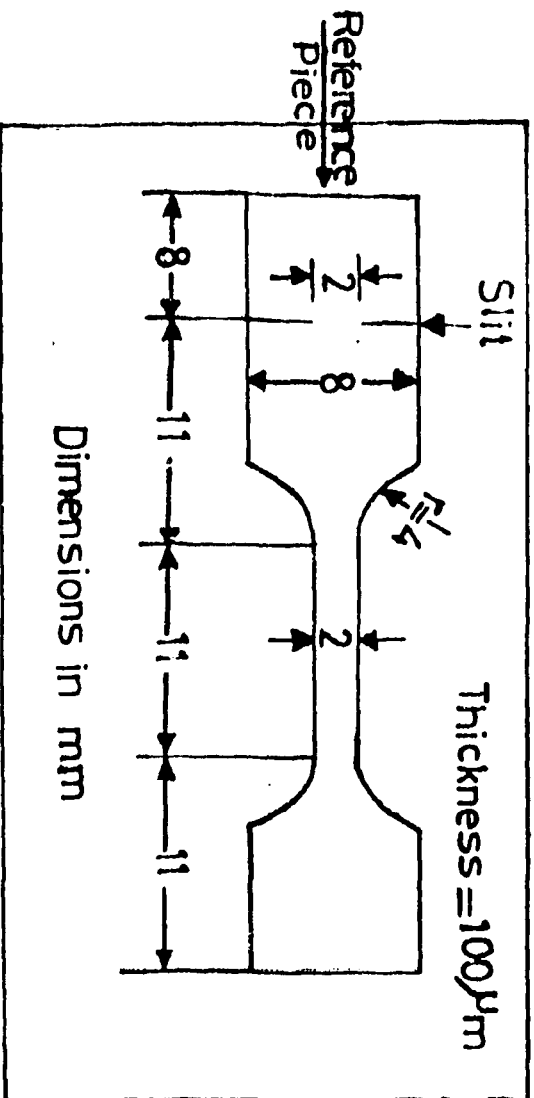


Fig. 5 Dimensions of creep specimen

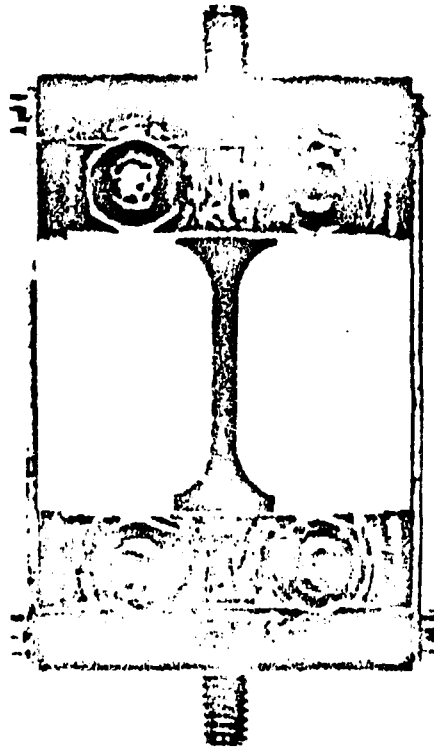
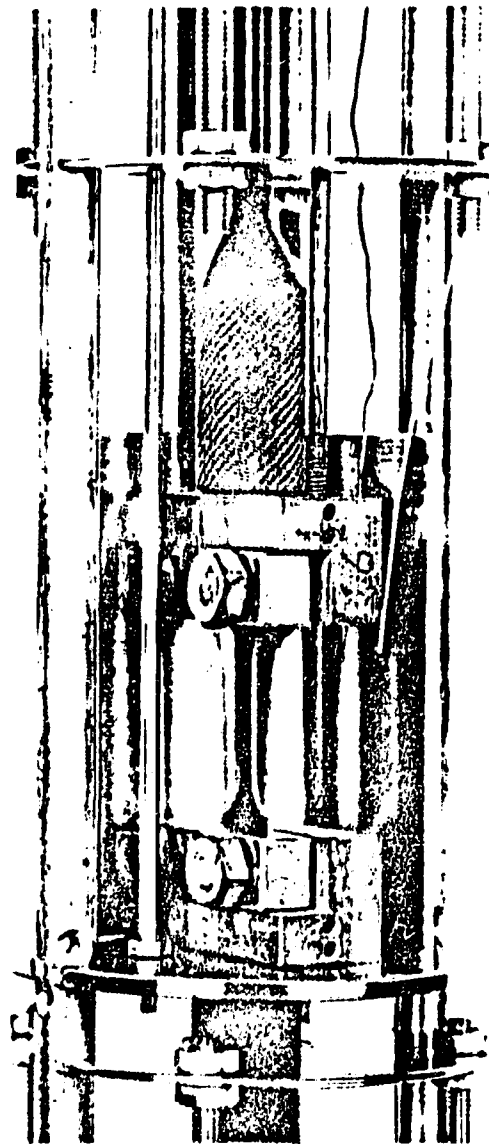


Fig. 6a : The creep sample mounted in the specimen holder outside the creep machine .



*Fig .6 b : The creep sample mounted in the
creep machine .*

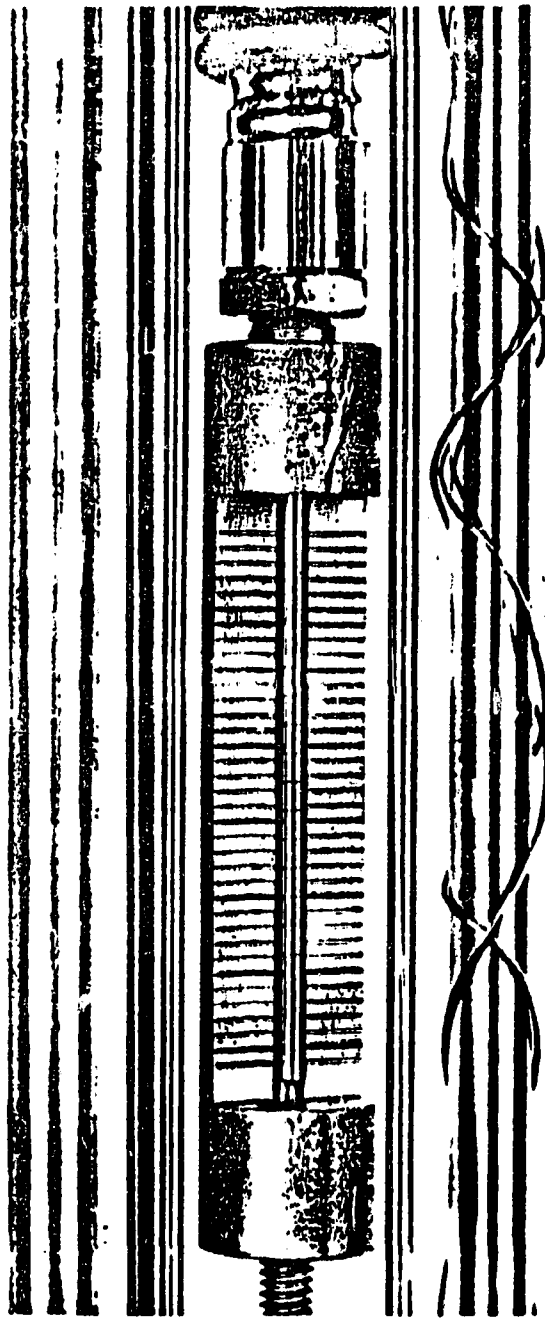


Fig: 7 : The load system

to 4-channel carrier frequency measuring amplifier for inductive transducers MBS 5207 made by Elan-Schaltelemente, Heuss, West Germany through vacuum penetrations.

The MBS 5207 Amplifier is connected to a two channel Chart Recorder model BBC SERVOGOR 120-11 to record the elongation occurs to the specimen during the whole test. Since the maximum permissible ambient temperature for the Inductive displacement transducers is 100°C so the creep machine should be long enough to avoid any heat transfer from the furnace therefore, small fan has to be fixed near the top of each column so that the transducers and the load system should be always kept at room temperature. As it has been previously mentioned for each creep machine, two W 10 K Inductive displacement transducers have been mounted out. One of them is connected to the upper part of the specimen holder by a stainless steel extensometer rod of approximately 40 cm long and the other one is connected to the lower part of the specimen holder through another stainless steel extensometer rod of about 44 cm long. For the correct load applied calculations the weight of the upper part of the specimen holder together with the two extensometer rods-together they wight approximately 50 gr grams - should be taken into account for the final and accurate load calculations. By using such a load, elongation measuring and recording systems the elongation of the specimen can be continuously and precisely measured to a sensitivity of $\pm 0.5 \mu\text{m}$ which is considered to be very high accuracy.

Figures 8 & 9 show that elongation-time calibration curves for these two creep machines which are in a good agreement with the data obtained from the universal machines for the same material of the same history crept at the same test conditions.

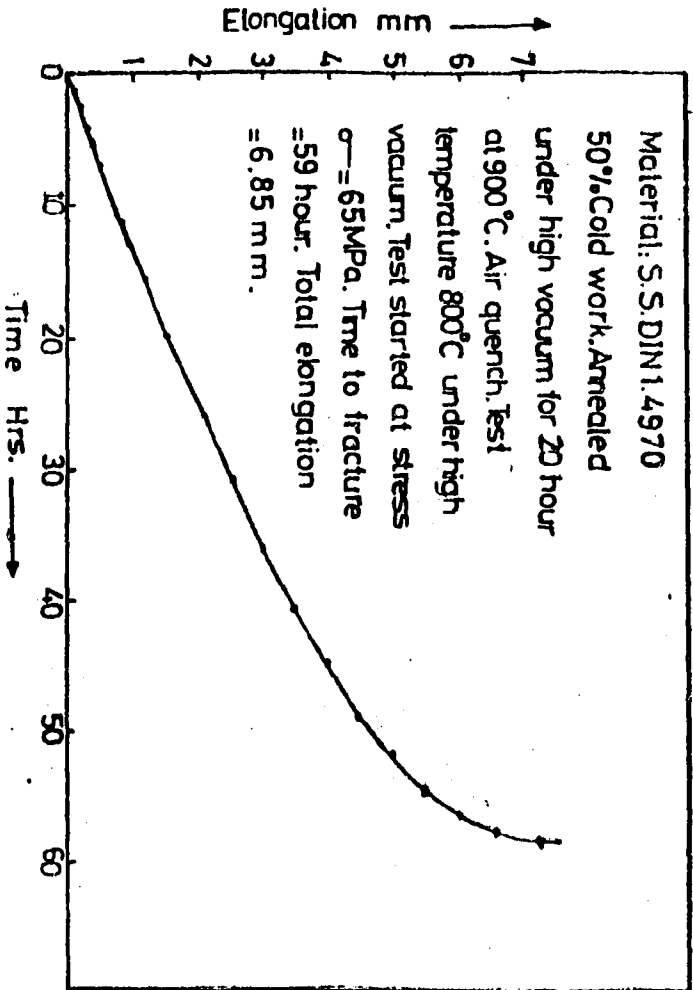


Fig. 8 Calibration curve for the creep machine 'Column 1'

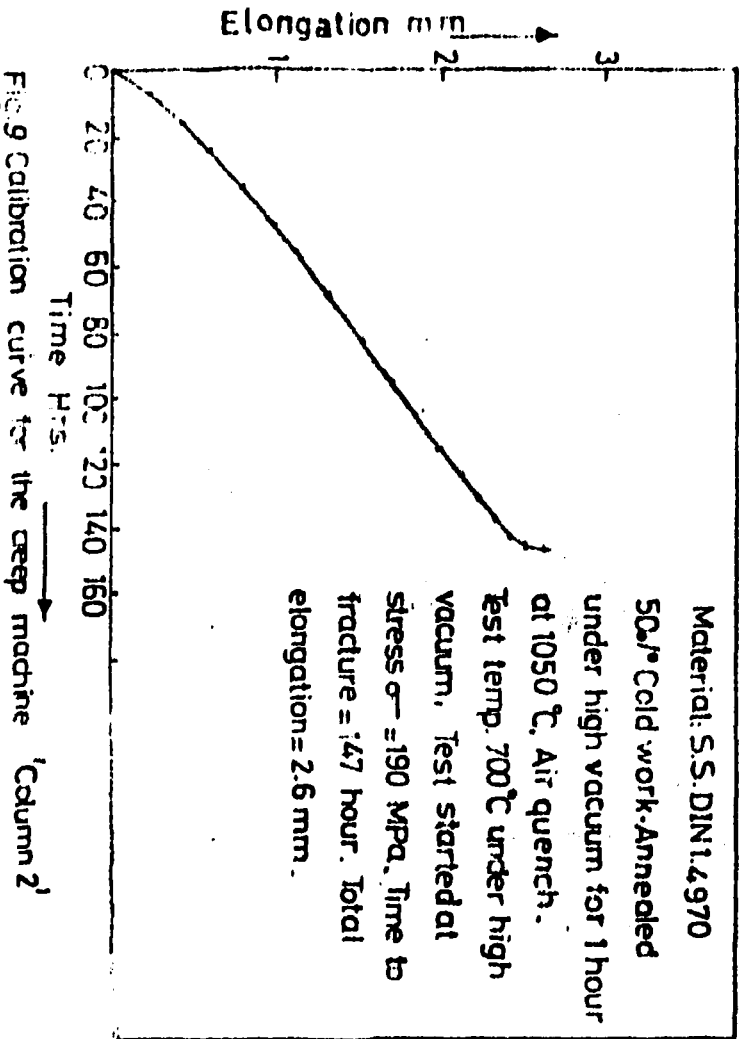


Fig. 9 Calibration curve for the deep machine 'Column 2'

III- CREEP BEHAVIOUR OF HELIUM IMPLANTED
AUSTENITIC STAINLESS STEEL

III-1. Experimental Procedure:

III.1.1. Sample preparation:

The present studies were conducted using tensile specimens prepared from austenitic stainless steel fuel pin tubes, of 7,6 mm diameter and 0.5 mm wall thickness, the chemical composition is shown in Table 1 as provided by the manufacturer Sandvik Sweden.

Table. 1
Chemical Analysis of the Sample Material wt.%

C	Si	Mn	Cr	Ni	Mo	Ti	N	B	Co	Ta	Cu
0.095	0.31	1.81	15.1	15.0	1.3	0.30	0.01	0.005	0.02	0.003	0.02

V
0.02

The tubes were split longitudinally 60% cold rolled to 200 µm and solution annealed at 1100°C for 1 hr (standard condition SC). They were subsequently cold rolled again to their final thickness of 100 µm (50% C.W.). From these strips the tensile specimens of 12 x 2 mm gauge area were cut by using spark erosion machine, Finally one batch of the specimens were aged at 900°C for 20 hr (Condition I) and the other batch aged at 1050°C for 1 hr (Condition II) All heat treatments were made in vacuum better than 10⁻⁶ using a turbomolecular pump.

III.1.2. Helium implantation

To study the phenomenon of He-embrittlement on austenitic stainless steel, tensile specimens from both conditions I and II were He-implanted to a concentration of 150 ppm using 28 Mev α - beam of the compact cyclotron in IFF-KFA, Jülich, West Germany. This technique provides a fast and convenient way of introducing helium with a minimum of side effects; a few hours of cyclotron irradiation result a uniform helium concentrations equal to those produced by several years of reactor exposure.

III.1.3. Creep tests:

Creep tests were carried out under vacuum better than 10^{-5} Torr using the above mentioned creep machines at 700°C and 800°C under different constant stress values for both of the unimplanted and helium-implanted tensile samples.

III.2 Results and Discussion of Creep Data:

The stress-rupture time diagrams are shown in Figs 10 and 11. The data are summarized in Table 2 for creep tests carried out at 700°C and 800°C for both thermal treatments of conditions I and II. Figures 10 and 11 show that rupture time at a certain stress value is less in condition I comparing with condition II for both test temperatures; at the same time condition I shows higher ductility with respect to condition II. Consequently one should expect slower average creep rate in condition II than in condition I which is clear from the data in Table 2.

Microstructure examinations using TEM (to be published) were carried out for samples of condition I crept at 700°C, the TEM micrographs showed new dislocation net works formed during creep test while for the samples of condition II crept at 700°C showed newly created dislocation networks

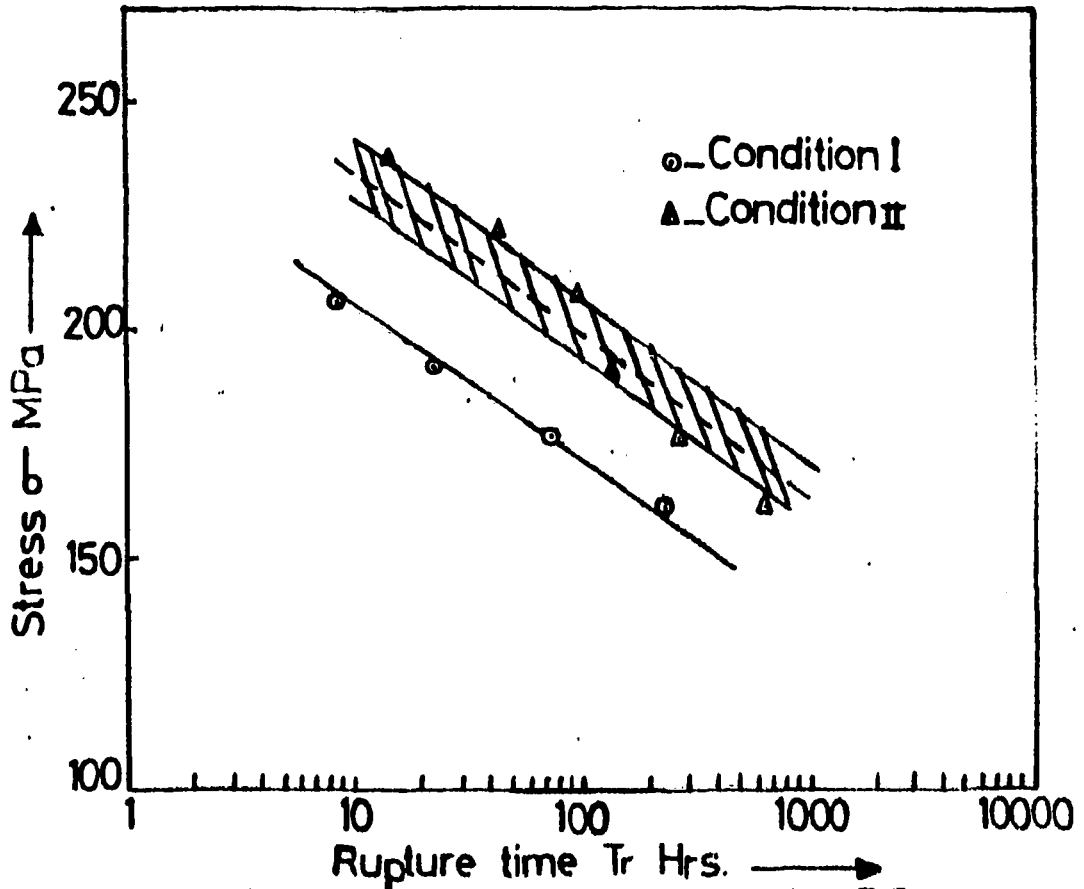


Fig.10 Stress vs. Log rupture time for S.S. crept at 700°C.

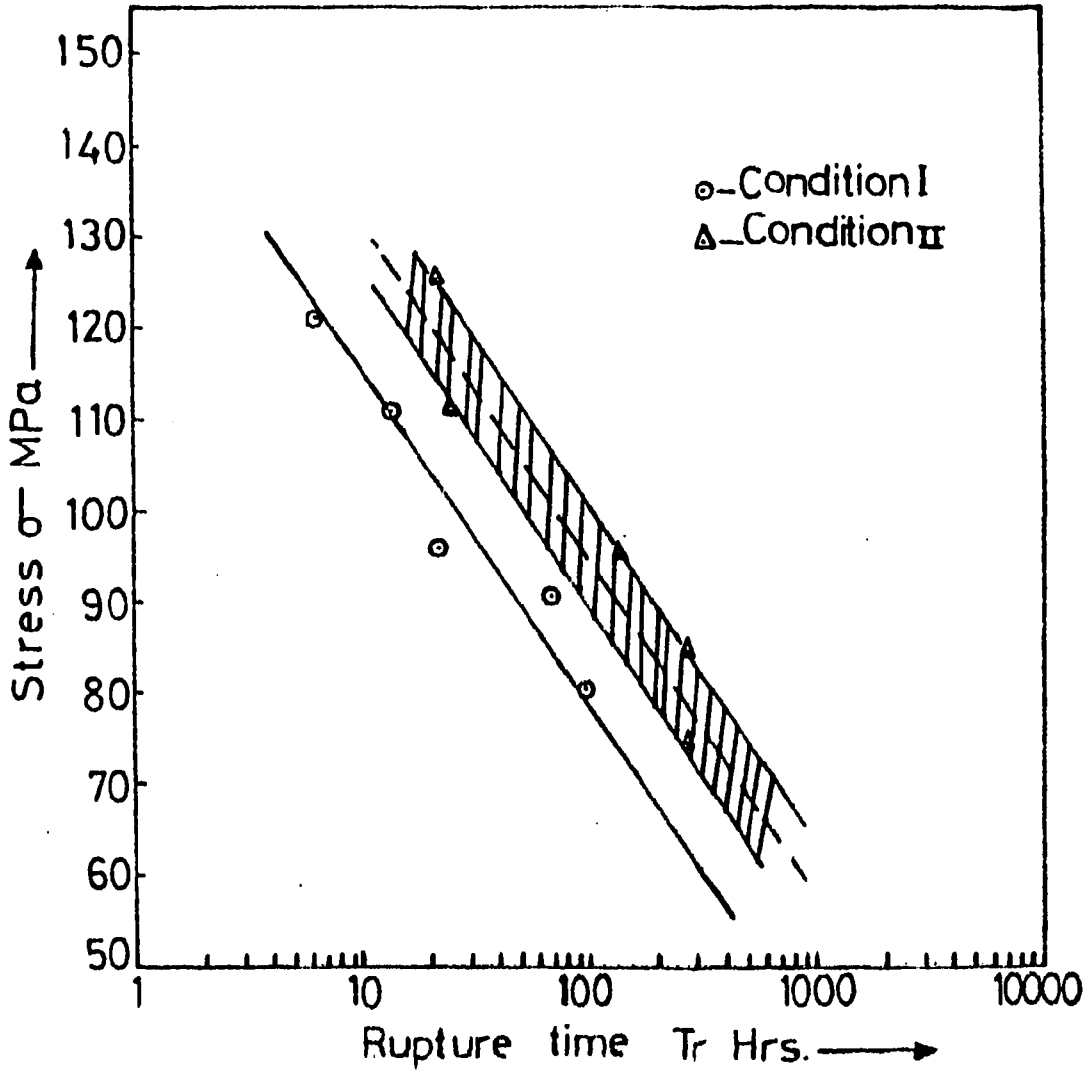


Fig.11 Stress vs. Log rupture time for S.S. crept at 800°C.

Table (2): Creep data for 1.4970 S.S. 50% C.W.

Annealed at 900°C for 20 hrs. (Condition I)							Annealed at 1050°C for 1 hr. (Condition II)						
Test Temp. °C.	Applied stress MPa	Rupture time hrs.	Total Elong. m.m.	Strain %	Average creep rate/hr.	Applied stress MPa	Rupture time hrs.	Total Elong. m.m.	Strain %	Average creep rate/hr.			
700	160	218	6.25	52.1	2.4×10^{-3}	160	583	3.5	29.16	5×10^{-4}			
800	95	20	6.5	54.1	2.7×10^{-2}	95	122.7	3.75	31.25	2.5×10^{-3}			
700	175	70.8	6.35	52.92	7.5×10^{-3}	175	250	2.57	21.4	8.5×10^{-2}			
800	110	12	8.45	70.4	5.78×10^{-2}	110	17.1	5.02	41.8	2.45×10^{-2}			
700	190	22	5.6	46.7	2.1×10^{-2}	190	132	4.2	35.5	2.6×10^{-3}			
500	80	91	7.4	61.7	6.75×10^{-3}	85	144.7	4.7	39.6	2.7×10^{-3}			
700	205	8.5	5.5	45	5.3×10^{-2}	205	90.66	3.1	25.6	2.8×10^{-3}			
800	120	5.5	7.85	65.42	1.19×10^{-1}	75	225	4.4	34.17	1.52×10^{-3}			
700	-	--	--	---	---	220	41.3	3.75	31.25	7.57×10^{-3}			
800	90	79	9.2	76.67	9.67×10^{-3}	-	--	--	---	---			
700	-	--	--	---	---	235	14	1.625	13.54	9.6×10^{-3}			
800	65	134	6.95	57.91	4.32×10^{-3}	-	--	--	---	---			
700	-	--	--	---	---	-	--	--	---	---			
800	60	661	10.6	88.13	2.21×10^{-3}	-	--	--	---	---			

and dispersed TiC particles of 100 \AA diameter. Thus the distribution of TiC precipitates and their interaction with the newly generated dislocations in specimens of condition II led to lower average creep rate.

Figs. 12 and 13 show the relationship between stress versus rupture time for samples of conditions I and II implanted with 150 ppm helium and crept at 700°C . The data are summarized in Table 3. From Figs. 12 and 13 and Table 3 it is shown that reduction of the elongation to fracture by factors between 2-4 and lower creep rates are observed. The presently accepted mechanism for explaining the loss in ductility is that helium bubbles weaken the grain boundaries of the material and thus promote the intergranular fracture.

In contrast to the effect of helium bubbles in weakening the grain boundaries it has a strengthening effect of the grains. The microstructure investigations using TEM for irradiated samples from condition I crept at 700°C shows helium bubbles at grain boundaries and dislocations with a large TiC particles in the centre, while for samples of condition II crept at 700°C indicated helium bubbles at TiC which were precipitated at dislocations or at the grain boundaries. More details on the microstructure investigations using TEM will be published later on.

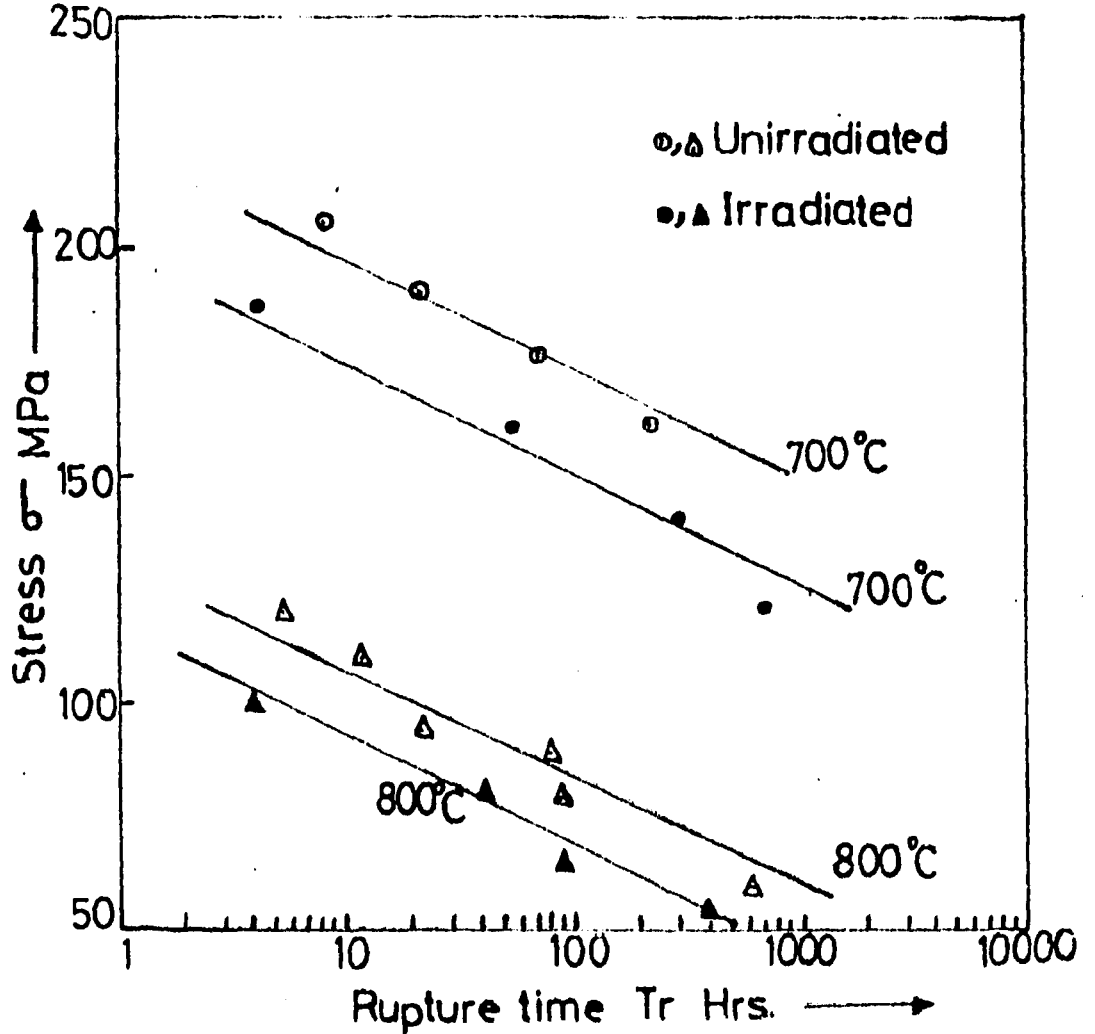


Fig.12 Stress vs. Log rupture time for annealed and 150 PPM He-implanted S.S. condition I crept at different temperatures.

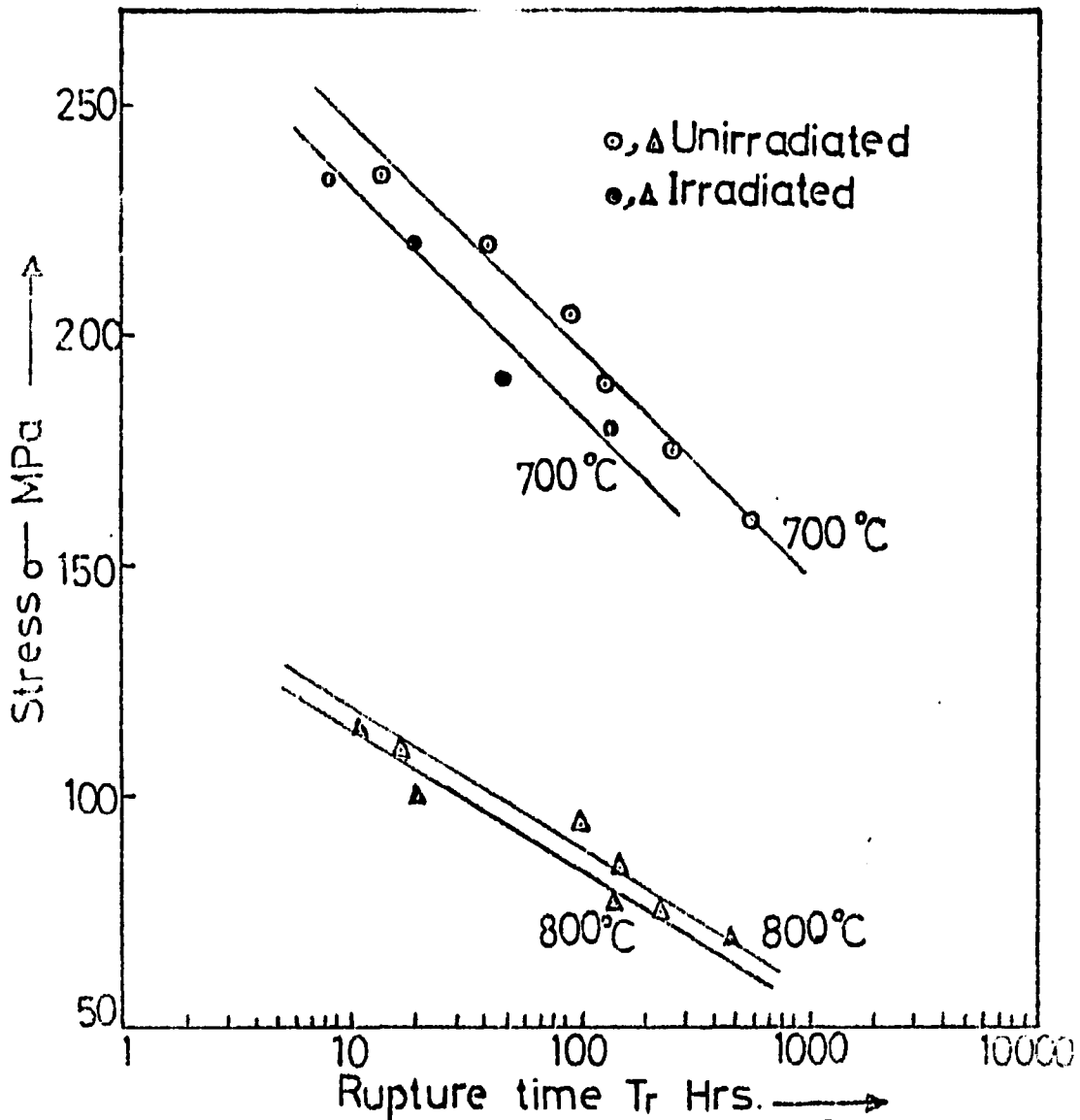


Fig.13. Stress vs. Log rupture time for annealed and 150 PPM He-impelanted S.S. condition II crept at different temperatures.

Table (3): Creep data for Irradiated 1.4970 S.S. 50% C.W.

Condition I + 150 ppm Helium Implantation						Condition II +150 ppm Helium Implantation					
Test Temp. °C.	Applied stress MPa	Rupture time hrs.	Total Elong. m.m.	Strain %	Average creep rate/hr.	Applied stress MPa	Rupture time hrs.	Total Elong. m.m.	Strain %	Average creep rate/hr.	
700	190	4.75	1.42	11.63	2.49×10^{-2}	190	44.7	1.54	12.8	2.87×10^{-3}	
800	100	4	1.62	13.5	2.38×10^{-2}	100	28	0.94	7.83	2.79×10^{-3}	
700	160	54.1	2.45	20.42	3.77×10^{-3}	175	598.6	2.4	20	3.34×10^{-4}	
800	80	42.4	2.75	22.52	5.4×10^{-3}	85	166	1.26	10.5	6.3×10^{-4}	
700	140	301	2.36	19.67	6.53×10^{-4}	185	167.5	1.37	11.42	6.82×10^{-4}	
800	65	88.7	2.7	22.5	2.54×10^{-3}	70	475.5	0.86	7.2	1.5×10^{-4}	
700	120	711	1.99	16.6	2.33×10^{-4}	207	89	2.23	18.6	2.09×10^{-4}	
800	55	412	2.89	24.08	5.35×10^{-4}	115	11	1.3	10.83	9.85×10^{-3}	
700	-	---	--	---	---	220	20	1.69	14.08	7.04×10^{-3}	
800	-	---	--	---	---	-	--	--	---	---	
700	-	---	--	---	---	235	8	2.07	17.25	2.16×10^{-2}	

REFERENCES

- [1] P. Greenfield, Creep of metals at high temperatures.
M & B monograph ME/9, Mills & Boon Limited London,
- [2] H. Morikawa, Jülich Rept. Jül 1290, April, 1976.
- [3] A.A. Sagües, H. Schroeder, W. Kesternich and
H. Ulmaier. J. Nucl. Mat 78 (1978) 289-298.
- [4] Ahmed A.Abou-Zahra and Herbert Schroeder, J. of
Nucl. Mat. 107(1982) 97-103.
- [5] W. Kesternich, M.K. Matta and J. Rothaut, J.Nucl.
Mat. (to be published).